Methyl-CpG binding domain 2 (Mbd2) is an Epigenetic Regulator of Autism-Risk Genes and Cognition

Elad Lax[1], Sonia DoCarmo[1], Yehoshua Enuka[2], Daniel M. Sapozhnikov[1], Lindsay A. Welikovitch[3], Niaz Mahmood[4], Shafaat A. Rabbani[4], Liqing Wang[5], Jonathan P. Britt[6], Wayne W. Hancock[5], Yosef Yarden[2], Moshe Szyf[1,7*]

1 Department of Pharmacology and Therapeutics, McGill University, Montreal, QC, Canada.

2 Department of Biological Regulation, Weizmann Institute of Science, Rehovot 76100, Israel.

3 Department of Neurology and Neurosurgery, McGill University, Montreal, QC, Canada.

4 Department of Medicine, McGill University Health Center, Montreal, QC, Canada.

5 Division of Transplant Immunology, Department of Pathology and Laboratory Medicine, and Biesecker Center for Pediatric Liver Diseases, Children's Hospital of Philadelphia and Perelman School of Medicine, University of Pennsylvania, Philadelphia, Pennsylvania, USA.

6 Department of Psychology, McGill University, Montreal, QC, Canada.

7 Sackler Program for Epigenetics & Psychobiology, McGill University, Montreal, QC, H3G1Y6, Canada.

*Corresponding author

Moshe Szyf, Department of Pharmacology and Therapeutics, McGill University, 3655 Sir William Osler Promenade, Montreal, QC, Canada. moshe.szyf@mcgill.ca

Abstract

The Methyl-CpG-Binding Domain Protein family has been implicated in neurodevelopmental disorders. The Methyl-CpG-binding domain 2 (Mbd2) binds methylated DNA and was shown to play an important role in cancer and immunity. Some evidence linked this protein to neurodevelopment. However, its exact role in neurodevelopment and brain function is mostly unknown.

Here we show that *Mbd2*-deficiency in mice (*Mbd2-/-*) results in deficits in cognitive, social and emotional functions. Mbd2 binds regulatory DNA regions of neuronal genes in the hippocampus and loss of *Mbd2* alters the expression of hundreds of genes with a robust down-regulation of neuronal gene pathways. Further, a genome-wide DNA methylation analysis found an altered DNA methylation pattern in regulatory DNA regions of neuronal genes in *Mbd2-/-* mice. Differentially expressed genes significantly overlap with gene-expression changes observed in brain of Autism Spectrum Disorder (ASD) individuals. Notably, down-regulated genes are significantly enriched for human ortholog ASD risk-genes. Observed hippocampal morphological abnormalities were similar to those found in individuals with ASD and ASD rodent models. *Mbd2* knockdown partially recapitulates the behavioral phenotypes observed in *Mbd2-/-* mice.

These findings suggest Mbd2 is a novel epigenetic regulator of genes that are associated with ASD in humans. Mbd2 loss causes behavioral alterations that resemble those found in ASD patients.

Introduction

Epigenetic modifications of the genome are long known to play a crucial role in normal brain function including a wide range of neuropsychological processes as well as in neuropsychological disorders [1]. The most studied epigenetic modification is DNA methylation, the addition of a methyl group to the DNA on a cytosine in a CpG dinucleotide context. DNA methylation in promoters and other regulatory regions suppress gene expression by interfering with transcription-factors and transcription machinery binding [2, 3]. An additional mechanism involves recruitment of members of a methylated-DNA binding proteins family (MECP2 and MBD1-6) which share a Methyl-CpG Binding Domain (MBD) [4, 5]. MECP2 and MBD2 were shown to recruit chromatin repressive complexes to genes and thus cause alterations in histone modification and silencing of gene-expression [6-8]. These proteins are highly expressed in brain tissues [9, 10].

The most extensively studied MBD protein is MeCP2 since mutations and duplications of this gene cause Rett syndrome [11, 12]. Some studies on the role of MBD1 suggest it has a role in neurodevelopment and neurodevelopmental disorders like autism [13]. In contrast, little is known about the roles of other MBD proteins in the brain.

Several studies associated MBD2 with neuropsychiatric disorders. An increased MBD2 DNA binding on the promoters of *BDNF*, *GAD1* and *RELN* genes was observed in post-mortem brains of schizophrenia and bipolar disorder patients [14]. There is evidence for rare nonsynonymous de novo mutations in *MBD2* identified in ASD [15-17]. Several studies found Copy Number Variants (CNV) at and around the genomic position of the *MBD2* gene (18q21.2) in ASD patients

(both deletions and duplications; see SFARI-CNV database: https://gene.sfari.org/database/cnv/). However, in these cases the CNVs span also other genes associated with ASD and related disorders, including *TCF4* (Pitt-Hopkins syndrome), *ASXL3* (Bainbridge-Ropers syndrome) and *SETBP1* (ID syndrome MIM #616078 and Schinzel-Giedion syndrome); thus confounding the role of Mbd2 deletions in the etiology of ASD.

MBD2-bound DNA regions are hypo-methylated in the prefrontal cortex of depressed suicide-completers [18]. In rat pups of low maternal care there is reduced Mbd2 expression in the hippocampus which corelates with reduced glucocorticoid receptor expression and elevated stress [19]. However, to date the mechanisms by which Mbd2 affect gene-expression and ultimately brain function and behaviors are unclear.

In the present study, we directly assessed the role of *Mbd2* in behavior using a knockout mouse model (*Mbd2-/-*). A comprehensive behavioral battery found cognitive, social and emotional deficits in Mbd2-/- mice. Since the behavioral abnormalities pointed to hippocampal functions we examined the molecular footprints of *Mbd2* in the hippocampus. We applied unbiased genome-wide approaches. Using ChIP-seq with an Mbd2-specific antibody we mapped the genome binding sites of Mbd2 and found that it binds methylated and unmethylated CpGS on and around many neuronal genes in the hippocampus as well as other genomic locations. Loss of Mbd2 binding in *Mbd2-/-* mice led to down-regulation of neuronal-gene expression. In contrast, up-regulated genes in *Mbd2-/-* mice were associated mostly to homeostasis and cell maintenance gene pathways. *Mbd2*-deficiency led to increased methylation on promoters and enhancers of neuronal genes, suggesting that Mbd2 affects DNA methylation status at neuronal genes and hence hippocampal genome functions. Furthermore, we found that differentially -

expressed genes were highly overlapped and correlated to differentially-expressed genes found in ASD individuals' brain. Down-regulated genes were highly enriched for ortholog ASD risk-genes implying an important role for Mbd2 in neurodevelopment and neuropsychiatric disorders.

Methods

Full details of all methods can be found in the supplementary file. All procedures were carried out in accordance with the guidelines set down by the Canadian Council of Animal Care and were approved by the Animal Care Committee of McGill University.

Results

Mbd2 is required for a range of cognitive, social and emotional behaviors

Previous studies on *Mbd2-/-* mice behavior found impaired maternal behaviors such as suboptimal feeding and delayed pup retrieval [20]. Hypoactivity, impaired nest-building behavior and mild spatial learning and memory impairments were found in male Mbd2-/- mice [21]. We further tested whether *Mbd2* is involved in behavior using additional behavioral tests. We tested both male and female mice and found no significant effect of sex for any of the behaviors measured (two-way ANOVAs, $p>0.05$ for main effect of sex and for interactions in all cases, FigS1 and FigS2). We therefore, grouped both males and females for subsequent experiments. There was no change in general locomotion in an open-field box (Fig 1A) or in other exploratory behaviors (speed, entries to the center of arena; Fig S3). Several forms of memory were tested as well. Short-term working-memory was assessed by spontaneous

alternations in Y-Maze and was found to be intact in *Mbd2-/-* mice (Fig 1E). Also, the number of arm entries did not differ between groups suggesting normal exploration behavior in *Mbd2-/-* mice (Fig 1E). In contrast, *Mbd2-/-* mice showed impaired memory-retention in the long-term object-location memory test compared to wild-type littermates and failed to explore the object in the novel location for more than chance levels (Fig1B). A previous study [21] did not find significant deficits in social behavior in *Mbd2-/-* mice using a three-chamber test which is a common test for sociability in mice. However, some mouse models for neurodevelopmental disorders show normal or near normal behavior in the three-chamber test while showing reduced sociability in the social interaction test [22-24] suggesting this test is more sensitive. We therefore used the social-interaction test and found that *Mbd2-/-* mice exhibited reduced social-interaction time (Fig 1C). We also measured anxiety-like behavior in the dark-light box (Fig 1D) and found that *Mbd2-/-* mice spent less time in the light compartment which indicates higher anxiety levels (Fig1D). Our findings support the hypothesis that Mbd2 is involved in regulating cognitive, social and emotional behaviors.

Landscape of Mbd2 binding in the hippocampus

We focused our analysis on the hippocampus since the behaviors affected in our study are known to involve hippocampal functions [25-29]. In addition, other members of the MBD protein family were shown to have an important role in hippocampal function [13, 30-32]. We performed Mbd2 ChIP sequence on wild type animals using input DNA to correct for non-specific reads. We identified 2436 Mbd2 peaks annotated to 1222 genes (with FDR<0.05). As expected, Mbd2 binds mostly to CpG-containing and GC-rich DNA regions (X^2=43.364; df=1, p=4.54E-11 and X^2=-1129.7; df=1, p=2.2E-16, respectively). Highly-enriched peaks were

observed in proximity to transcription-start-sites (Fig2A and FigS4A). Interestingly, de-novo motif discovery found the transcription-factors E2F7 (p=1E-197) and Zic3 (p=1E-143) to be highly enriched in hippocampal Mbd2 peaks (FigS4B). The E2F family and Zic family have been previously reported to have a role in neurogenesis and brain development [33-35]. We also compared our data to publicly available ChIP-Seq data of the mouse hippocampus histone-marks [36]. As expected, Mbd2 bound overall to more repressive histone-marks (mostly H3K9me3) than to active histone-marks. However, a subset of the peaks was bound to both active and repressive histone-marks. This might imply that either Mbd2 binds sites that are bivalently marked in the same cell or that Mbd2 binds DNA regions that have different chromatin states in different cell populations within the hippocampus (Fig2B-C). Mbd2 co-occupancy with histone-marks on promoters, 5' UTRs and gene-bodies (mostly exons) was enriched for active histone-mark and depleted from repressive histone-marks (Fig2D). Pathway-analysis by GO-enrichment found that Mbd2 binds many neuronal- and brain-related pathways such as: trans-synaptic signaling, synapse organization and behavior (Fig2E and FigS5A). These pathways also showed good clustering as GO-networks (FigS5B) and protein-protein interactions analysis found forebrain-development and axon-guidance as the top 2 annotations (log10p= -6.3 and -5.6, respectively) further supporting a role for Mbd2 in neuronal development and function.

We selected 15 peaks of Mbd2 that were associated with promoters or enhancers in neuronal-related genes for further validation and for determining the impact of Mbd2 binding loss on transcription-initiation (see Table S1 for genomic coordinates of validated peaks). Quantitative-ChIP PCR confirmed binding of Mbd2 to these regions and loss of binding in *Mbd2-/-* mice

(Fig2F). We then determined whether loss of Mbd2 binding in promoters or enhancers in *Mbd2-/-* mice affects transcription onset. *Mbd2*-deficiency resulted in reduced transcription onset since occupancy of RNA-polymerase phosphorylated on Serine5; (RNApolII(SP5)) the form found on promoters upon transcription-initiation [37, 38] was reduced in *Mbd2-/-* mice. Interestingly, this was associated with increased abundance of histone-mark (H3K4me1) marking enhancers in *Mbd2-/-* hippocampi (Fig2G-H). H3K4me1 modification marks active as well as inactive enhancers [39, 40]. H3K4me1 peaks that are flanking the TSS were shown to exhibit a peak-valley-peak pattern. The valley usually overlaps with transcription-initiation and RNApolII(SP5) peaks [41] reflecting a nucleosome-free zone and thus reduced histone presence and reduced signal for the histone-marks, which is prerequisite for transcription-initiation [42]. In transcriptionally inactive genes H3K4me1 peaks cover the entire TSS forming one continuous peak centered at the TSS and overlapping with the RNApolII(SP5) peaks. The increase of H3K4me1 concurrently with reduction of RNApolII(PS5) binding at the same position in *Mbd2-/-* mice is consistent with inhibition of transcription onset in response to *Mbd2* deficiency. These data suggest that Mbd2 is involved in activation of transcription turn on in these neuronal-specific promoters.

Mbd2 is required for expression of neuronal genes

To further elucidate the role of Mbd2 in hippocampal gene-expression we delineated the transcriptomes of wild-type and *Mbd2-/-mbd2-/-* mice using RNA-Seq. We found 2907 genes to be differentially-expressed (FDR<0.05), of which 1590 genes were up-regulated, and 1317 gene were down-regulated in *Mbd2-/-* mice (Fig3A, and FigS6 for validations). Pathway-analysis by GO-enrichment found a robust down-regulation of neuronal-related pathways such as neuron-

projection development, trans-synaptic signaling and behaviors (Fig3B and Fig S7A) which were highly organized in clusters based on clustering analysis of the GO-networks (Fig S7B). In striking contrast, the same analyses applied to up-regulated genes revealed mostly homeostasis and metabolism related pathways with no enrichment of neuronal-related pathways (Fig 3C and Fig S8A). GO-network analysis revealed poor clustering of the differentially-expressed genes in these pathways (Fig S8B).

Next, we determined whether the differentially-expressed genes were interacting with Mbd2 by overlapping the Mbd2 ChIP-seq and RNA-seq results. A significant fraction of the down-regulated genes had Mbd2 peaks annotated to them (85 genes; p=1.8E-9; hypergeometric-test) while fewer up-regulated genes (55) had annotated Mbd2 peaks (p=0.31; hypergeometric-test). Meta-analysis of the overlapping ChIP-seq and RNA-seq enriched pathways by unsupervised clustering found that the top downregulated pathways in *Mbd2-/-* mice were trans-synaptic signaling, behavior and synaptic organization (Fig S9). These findings are consistent with a role for Mbd2 in regulating neuronal gene-expression.

The impact of *Mbd2* depletion on the DNA methylation landscape

MBD proteins are “readers” of DNA methylation and bind specifically to methylated DNA [4, 43]. However, it is possible that they also play a role in maintaining DNA methylation/demethylation landscapes as has been previously proposed. Previous studies in T-regulatory cells using *Mbd2-/-* animals have suggested that depletion of *Mbd2* causes hypermethylation of regulatory regions which in turn results in downregulation of gene-expression [44]. Therefore, we tested whether M*bd2*-deficiency would alter the landscape of

DNA methylation in the hippocampus. We mapped with targeted-bisulfite-sequencing the methylation state of regulatory DNA regions (promoters and enhancers, see methods) in the hippocampi of M*bd2-/-* and wild-type mice at a single-base resolution. A global methylation analysis revealed that Mbd2 binding regions defined in wild-type mice by ChIP-seq were hypermethylated in *Mbd2-/-* mice (Fig 3D). Hypermethylation in response to *Mbd2* depletion was observed also in a genome-wide scale analysis which examined DNA outside the regions that bind Mbd2 ($p<2.2E-16$, K-S test, Fig S11C). The fact that changes in DNA methylation occur in regions that do not bind Mbd2 suggests *Mbd2*-deficiency could affect DNA methylation indirectly. We therefore examined our RNA-seq data for expression levels of methylated-CpG readers and modifiers. We found a significantly reduced expression of *Tet2*, *Dnmt3a*, *Mbd1* and *Mecp2* in *Mbd2-/-* mice (Fig S10). The reduced expression levels of enzymes which promote de-novo DNA methylation (*Dnmt3a*) and de-methylation (*Tet2*), together with the reduced levels of methyl-CpG binding proteins (*Mbd1* and *Mecp2*) likely contributed to changes observed in the landscape of DNA methylation in *Mbd2-/-* mice. Taken together these data suggest that loss of *Mbd2* affects DNA methylation in both directions. An analysis of the sequence properties of Mbd2-dependent DNA methylation suggests that *Mbd2*-deficiency results in increased methylation of low to intermediate methylated CpGs (10-40% methylation) but highly methylated CpGs (>40% methylation) are unaffected as expected if Mbd2 prevents hypermethylation. Partially methylated genes represent a group of genes that are heterogeneously methylated and possibly heterogeneously expressed across hippocampal nuclei. Mbd2 might be regulating the state of methylation of these genes.

We also analyzed differential-methylation at single CpG resolution. At this resolution differential-methylation analysis (at least 10% difference, FDR<0.05; Fig S11A) revealed 323 differentially-methylated CpGs, with 133 hypo-methylated CpGs (annotated to 103 genes) and 190 hyper-methylated CpGs (annotated to 119 genes) (differential-methylation data (p<0.001) is detailed at Table S2). This finding also supports a significant overall hypermethylation in *Mbd2-/-* mice hippocampus (p=0.0018, binomial-test). For pathway-analysis, we applied a more lenient significance cut-off for our data (p<0.001) resulting in 3005 differentially-methylated CpGS (1519 hypo-methylated and 1486 hyper-methylated). Next, we focused the analysis on CpGs located on promoters (±1000bp from TSS). We found 494 hypo-methylated CpGs located in 460 gene-promoters and 476 hyper-methylated CpGs located in 434 gene-promoters (Fig S11A). Pathway-analysis for differentially-methylated gene-promoters revealed adrenergic receptor signaling and sodium- and metal- ion transports as the top three hyper-methylated pathways (-log10p-values: 4.86, 4.16 and 3.42, respectively). In contrast, the top hypo-methylated pathways were not specifically related to neurons or brain functions, although neuronal ion-channel clustering and positive regulation of sodium ion-transport pathways were enriched (-log10p-values: 3.289 and 3.280, respectively) (Fig S11E-F). Overall, this analysis suggests an enrichment of hyper-methylated genes related to neuronal gene-pathways in *Mbd2-/-* mice hippocampi.

Next, we assessed how binding of Mbd2 affects single CpG DNA methylation in Mbd2-bound genes. We analyzed the changes in DNA methylation levels for CpG (with at least 10% change and p<0.001) annotated to Mbd2-bound genes and found significantly more genes had hyper-methylated CpGs (p=0.0339, binomial test, Fig 3E). When analyzing only the subset of these

CpGs which were located directly at Mbd2 binding peaks we found in almost all cases (~95%) hyper-methylation of these CpGs (p<1E-8, binomial test, Fig 3F). This is consistent with a role for Mbd2 binding in maintaining a hypomethylated state.

To assess the relation between promoter DNA methylation and gene-expression we determined the correlation between methylation and expression. We found a significant linear inverse correlation between promoter DNA methylation and gene-expression (Fig3G), supporting a role for DNA methylation in gene-repression in the hippocampus. Unexpectedly, a subset of differentially-methylated CpGs in promoters showed positive correlation between expression and methylation. We explored this finding by analyzing DNA motifs around these CpGs. While CpGs with inverse correlation (n=66) had no significantly enriched motifs; CpGs with positive correlation (n=40) had 3 enriched motifs (p-values= 0.015-0.025). These enriched motifs were highly similar to known motifs of the KLF and SP transcription-factor families with top similarities to: KLF12, KLF14, SP3 and SP8 (FigS 11D). The KLF and SP transcription-factors are known to prefer binding to methylated-DNA (KLF) or to be unaffected by DNA methylation (SP) [45]. This finding suggests that genes whose methylation status does not correlate inversely with their expression, are regulated by transcription-factors that are not inhibited by DNA methylation.

We also validated our DNA methylation analysis results by targeted-sequencing of bisulfite-converted PCR amplicons of nine Mbd2 binding regions each of which annotated to a different gene (See Table S5 for delineation of the regions). Methylation levels in these regions strongly correlated with the levels obtained in the genome-wide capture sequencing analysis (range of Pearson's r=0.884 - 0.913; Fig S12A-B). Loss of *Mbd2* promoted bi-directional alterations in DNA

methylation status with enhanced hyper-methylation, as observed before (Fig S12C-D). Overall there was a significant hyper-methylation in *Mbd2-/-* samples (Fig S12E) as was observed in the genome-wide capture-sequencing.

Differentially-expressed genes in *Mbd2-/-* mice are associated with differentially-expressed genes in ASD individuals' brains and ASD risk genes

Other MBD proteins were associated with ASD [12, 13, 30, 32, 46] and the presentation of behavioral abnormalities in *Mbd2-/-* mice described above resembles some of the observed symptoms of ASD. Therefore, we sought to explore the potential relation between our gene-expression findings and those found in post-mortem brains from neurodevelopmental disorders patients. We compared our data to the recently released cortex transcriptomic data from the psychENCODE consortium [47] for ASD, schizophrenia and bipolar disorder.

We found a highly significant overlap between differentially down- and up- regulated genes in Mbd2-/- mice and individuals with ASD (Fig 4A). We also found a weak, though significant, overlap between down-regulated (but not up-regulated) genes in Mbd2-/- mice and down-regulated gene in schizophrenia patients (Fig 4A). We did not find any significant overlap with bipolar disorder differentially expressed genes (Fig 4A). Using correlation analysis, we found a significant positive correlation of gene-expression fold-change levels between Mbd2-/- mice and ASD individuals but not between Mbd2-/- mice and schizophrenia or bipolar disorder patients (Fig 4B).

Next, we compared our gene-expression data with that of two human ASD risk-genes databases: a study by Sanders et al. [48]and the SFARI-gene database (see methods). We found

a robust overlap between ASD-risk genes and down-regulated genes in *Mbd2-/-* mice. Twenty-four (~37%) out of 65 ASD risk genes (FDR<0.1) found by Sanders et al. [48]were down-regulated in *Mbd2-/-* mice (p=2.47E-12, hypergeometric-test, Fig5A and table S3). In contrast, only 3 genes from the 65 gene-list were up-regulated in *Mbd2-/-* mice (p=0.91 hypergeometric-test). The 24 down-regulated genes common to mice and humans also formed a significant protein-protein interaction network (p= 8.12E-6, Fig S13A) with some of the top GO pathway annotations related to "regulation of biological and cellular processes" and "nervous system development" (Table S4).

Next, we compared our RNA-seq results to the SFARI-gene list of ASD-associated genes which contains all known human genes associated with ASD. Here again, out of 951 human genes associated with ASD, 125 (13.14%) were down-regulated (p=8.8E-13, hypergeometric-test, Fig 5B and table S3) while only 44 were up-regulated in *Mbd2-/-* mice (4.62%, p=0.99, hypergeometric-test, Fig 5B and table S3). Analysis of Mbd2-regulated ASD-associated gene-lists revealed significant protein-protein interactions enrichments. The 125 down-regulated genes which appears also in the SFARI ASD-associated gene-database projected into a significantly enriched protein-protein network (p<1E-16; Fig S14A) with "nervous-system development" and "modulation of excitatory postsynaptic potential" as the most enriched GO-pathways within the network (p=5.84E-15 and p=2.14E-13 respectively, table S4). The 44 up-regulated genes which appear also in the SFARI ASD-associated gene-database projected into a significantly enriched protein-protein network (p=0.00559; Fig S14B) with "dendritic spine morphogenesis" and "modulation of excitatory postsynaptic potential" as the most enriched GO-pathways within the network (p= 0.00162 in both cases, table S4).Taken together, these

transcriptomic and genomic cross-species comparative analyses suggest that Mbd2 might serve as an up-stream regulator to many ASD-associated genes. This is in line with previous observations that showed regulatory roles for Mbd2 in liver, breast and prostate cancer genes in cancer cell lines [49-51], NGFIA in hippocampal cells [19] and *Foxp3* gene [44] in regulatory T-cells. We further analyzed the protein levels of few members of the protein-protein network of ASD-risk genes and found reduced protein levels of these genes in *Mbd2-/-* mice (Fig 5C) which agrees with the mRNA reduction we observed before.

Morphological changes in the hippocampus were observed as well. We found increased neuron count in the CA1 and CA2 regions of the hippocampus (Fig 5D and Fig S15), reduced CA1 thickness and a negative correlation between neuron-size and neuron count (CA1) and between neuron-size and thickness (CA2 and total hippocampus). These changes indicate an increased neuronal density and reduced thickness in the hippocampus of *Mbd2-/-* mice, phenomena which were previously reported in ASD rodent models and human subjects [52-54]. Increased neuronal density was also observed in the cortex of children with autism [55].

Hippocampal Mbd2 down-regulation impaired cognitive and emotional behaviors

Next, we asked whether hippocampal Mbd2 is casually involved in regulation of behaviors which are impaired in adult *Mbd2-/-* mice. We therefore examined whether Mbd2 down-regulation in adult mice affects some or all of the behavioral changes seen in *Mbd2-/-* mice which lacked the gene both during embryogenesis and post-natal development. To this end, we constructed several shRNA lentiviruses which targeted *Mbd2* mRNA (sh-*Mbd2*; Fig S16A-C). The construct which was the most active in *Mbd2* depletion as tested *in-vitro* was infused *in-vivo*

into the hippocampus of adult wild-type mice to knockdown Mbd2 in-vivo (Fig 6A-B). GFP-expressing-cells were found near the injection site and up to the dentate gyrus and stratum radiatum of CA3 (S16D). Following the infusion and recovery we tested the mice in the same behavioral tests that were found to be abnormal in *Mbd2-/-* mice. Down-regulation of Mbd2 did not affect locomotion in an open-field (Fig 6C) or interaction time in the social-interaction test (Fig 6E). However, Mbd2 down-regulation resulted in failure of treated mice to remember location of objects in the object-location-memory test. While control mice explore the object in the novel-location significantly more than the familiar location ($p<0.05$, one-sample t-test), sh-*Mbd2*-treated mice did not explore the object in the novel location any longer than chance level ($p>0.05$, one-sample t-test, Fig 6D). In the Dark-Light-Box test, sh-*Mbd2*-treated mice showed increased anxiety expressed as reduced time in the light compartment (Fig 6F). Taken together, these results show that knockdown of hippocampal Mbd2 in adult mice recapitulate two of the behavioral abnormalities found in *Mbd2-/-* mice but not the social interaction deficiency.

Discussion

There is growing evidence for the crucial role of epigenetic mechanisms in neuropsychological disorders and CNS function. In this study, we tested the role of Mbd2, a methylated-CpG binding protein, in gene-expression and brain function. Mbd2, like other MBD proteins, serves as a “reader” of the epigenome [4] translating DNA methylation marks into gene-expression regulation mechanisms. It has previously noted that loss of Mbd2 results in behavioral deficits such as impaired maternal care, poor nest building and mild memory impairment [20, 21].

Here we report that loss of Mbd2 results in cognitive, social and emotional deficits. Taken together these results imply a role for Mbd2 in normal brain function. Two of the phenotypic findings were replicated by hippocampus-specific down-regulation of Mbd2 in wild-type mice, providing further evidence for the causal role of hippocampal Mbd2 in regulating behavioral phenotypes including long-term spatial memory and emotional control. Social interaction was not affected by *Mbd2* knockdown. It is possible that the level of inhibition of Mbd2 achieved by lentiviral knockdown was insufficient to affect social interaction. Alternatively, hippocampal Mbd2 might play a developmental role in social interaction behaviors and might not be required for maintenance of this behavior in adults.

Since the effects of *Mbd2*-deficiency on behavior were broad and related to hippocampal function [25-29], we used genome-wide approaches to define the landscape of Mbd2 binding in the hippocampus of normal animals and then determined how its deficiency affects the landscapes of DNA-methylation and gene-expression using *Mbd2-/-* mice. Consistent with an important role in brain function as detected by the behavioral assays presented here, pathway-analyses revealed a highly clustered and networked enrichment of genes relating to cognitive functions and brain development such as trans-synaptic signaling, synapse organization and behavior.

Mbd2 regulates gene-expression by binding to methylated CpGs in DNA [56]. MBD proteins are generally considered to have a repressive role on gene-expression by interacting with chromatin modification inactivating complexes [57]. However, evidence suggests other MBD

proteins are involved in gene-expression in more than one way. For example, hypothalamic Mecp2 dysfunction led to robust changes in gene-expression with 85% of the genes activated by Mecp2; a process possibly mediated by the interaction of the transcriptional-activator Creb1 with Mecp2 in binding gene-promoters and regulatory regions [58]. Similarly, Mecp2 promotes the expression of *Fopx3* in regulatory T-cells (Treg), a key regulator of Treg function, by collaborating with Creb1 [59]. Neuronal Mbd1 was also found to have a mixed effect on gene-expression in the hippocampus with more than half of the genes down-regulated in *mbd1-/-* mice, many of them associated with neurogenesis [60]. Mbd2 was previously shown to be involved in both suppression of promoters through recruitment of transcriptional-repressors, and in activation of promoters in cancer cells and the hippocampus through recruitment of transcriptional-activators [19, 49-51] such as CBP and NGFIA [19, 51, 61] as well as by targeting DNA demethylation [62, 63] possibly through recruitment of oxygenases such as Tet2 [44] .

Consistent with these data we found evidence for the bimodal function of Mbd2 in the hippocampus. *Mbd2*-deficiency resulted in both gene activation and repression as well as hypermethylation and hypomethylation. Interestingly, the neuronal specific functions seem to be mainly repressed and hypermethylated by *Mbd2*-deficiency, suggesting a mostly activating role for Mbd2 at neuronal-specific genes. This is supported by the observation that Mbd2 localizes to promoter and transcription start regions.

To further examine the role of Mbd2 in transcriptional activation/repression, we examined several promoters and enhancers that bind Mbd2 and examined the consequences of *Mbd2*-deficiency on transcription-initiation. Most of the genes examined had reduced RNApolII(PS5)

occupancy and increased H3K4me1 masking of the transcription-initiation region indicating reduced transcription-initiation upon *Mbd2*-deficiency.

Both genetic and environmental factors are believed to be involved in the etiology of ASD and other neurodevelopmental disorders. DNA methylation has been proposed as an epigenetic interface which links environmental factors to genomic susceptibility in ASD [64, 65] and neurodevelopment [66]. MBD proteins as readers of DNA methylation are therefore potential mediators which translate the altered DNA methylation landscape into gene-expression and ultimately behavioral changes. While the involvement of MBD2 in psychiatric disorders was previously suggested [14, 16, 67], our study is the first to provide a possible mechanism. Interestingly, the list of genes that we found here to be Mbd2-dependent was significantly enriched in ASD-associated genes according to brain transcriptomic and GWAS studies [47, 48]. Moreover, the behavioral phenotypes that we and others have characterized in Mbd2-/- mice resemble several of the phenotypes frequently observed in ASD patients such as social-avoidance, anxiety and deficits in learning and memory. This is accompanied by morphological changes in the hippocampus similar to those previously reported in ASD patients and ASD rodent models such as increased number of neurons [52, 55] accompanied by reduced thickness of hippocampal sub-regions [53, 54]. It is therefore possible that *Mbd2*-/- mice have impaired neuronal development which results in an increased number of presumably immature neuron but less mature neurons. This pattern has been described before in *Mbd1-/-* mice [13, 60].

Taken together, our findings further highlight the importance of MBD proteins in neuropsychological disorders. Our findings also provide evidence that Mbd2 is a regulator of neuronal gene-expression, brain morphology and behavior.

Acknowledgements

The work was funded by a grant (PSR-SIIRI) from the Ministère du Développement économique et de l'Innovation, Gouvernement du Québec and a grant from the Canadian Institute for Health Research PJT-159583. EL was funded by the Richard and Edith Strauss Canada Fund post-doctoral fellowship. SDC is the holder of the Charles E. Frosst/Merck Research Associate position. LAW is the recipient of a Doctoral Training Fellowship from the Fonds de recherche du Québec – Santé. The authors wish to thank Dr. David Cheishvili for critical discussion as well as to Bruktawit Maru, Helen Liu, Isabel Kalaycioglu and Stéphanie L'Écuyer for their technical help. Capture and hybridization was performed by the Institut de recherches cliniques de Montréal (Montreal, Canada; licensed by Roche Nimblegen). Next-generation sequencing was performed at Genome-Quebec (Montreal, Canada; licensed by Illumina).

Conflict of Interest

All authors declare they have no conflict of interest.

References

1. Sweatt, J.D., *Neural plasticity and behavior - sixty years of conceptual advances.* J Neurochem, 2016. **139 Suppl 2**: p. 179-199.
2. Lister, R., et al., *Human DNA methylomes at base resolution show widespread epigenomic differences.* Nature, 2009. **462**(7271): p. 315-22.
3. Weber, M., et al., *Distribution, silencing potential and evolutionary impact of promoter DNA methylation in the human genome.* Nat Genet, 2007. **39**(4): p. 457-66.
4. Du, Q., et al., *Methyl-CpG-binding domain proteins: readers of the epigenome.* Epigenomics, 2015. **7**(6): p. 1051-73.
5. Jorgensen, H.F. and A. Bird, *MeCP2 and other methyl-CpG binding proteins.* Ment Retard Dev Disabil Res Rev, 2002. **8**(2): p. 87-93.
6. Baubec, T., et al., *Methylation-dependent and -independent genomic targeting principles of the MBD protein family.* Cell, 2013. **153**(2): p. 480-92.
7. Nan, X., F.J. Campoy, and A. Bird, *MeCP2 is a transcriptional repressor with abundant binding sites in genomic chromatin.* Cell, 1997. **88**(4): p. 471-81.
8. Ng, H.H., et al., *MBD2 is a transcriptional repressor belonging to the MeCP1 histone deacetylase complex.* Nat Genet, 1999. **23**(1): p. 58-61.
9. Fan, G. and L. Hutnick, *Methyl-CpG binding proteins in the nervous system.* Cell Res, 2005. **15**(4): p. 255-61.
10. Hendrich, B. and A. Bird, *Identification and characterization of a family of mammalian methyl-CpG binding proteins.* Mol Cell Biol, 1998. **18**(11): p. 6538-47.
11. Amir, R.E., et al., *Rett syndrome is caused by mutations in X-linked MECP2, encoding methyl-CpG-binding protein 2.* Nat Genet, 1999. **23**(2): p. 185-8.
12. Moretti, P. and H.Y. Zoghbi, *MeCP2 dysfunction in Rett syndrome and related disorders.* Curr Opin Genet Dev, 2006. **16**(3): p. 276-81.
13. Zhao, X., et al., *Mice lacking methyl-CpG binding protein 1 have deficits in adult neurogenesis and hippocampal function.* Proc Natl Acad Sci U S A, 2003. **100**(11): p. 6777-82.
14. Dong, E., et al., *DNA-methyltransferase1 (DNMT1) binding to CpG rich GABAergic and BDNF promoters is increased in the brain of schizophrenia and bipolar disorder patients.* Schizophr Res, 2015. **167**(1-3): p. 35-41.
15. Gandal, M.J., et al., *Shared molecular neuropathology across major psychiatric disorders parallels polygenic overlap.* Science, 2018. **359**(6376): p. 693-697.
16. Li, H., et al., *Mutation analysis of methyl-CpG binding protein family genes in autistic patients.* Brain Dev, 2005. **27**(5): p. 321-5.
17. Coe, B.P., et al., *Neurodevelopmental disease genes implicated by de novo mutation and copy number variation morbidity.* Nat Genet, 2019. **51**(1): p. 106-116.
18. Nagy, C., et al., *Astrocytic abnormalities and global DNA methylation patterns in depression and suicide.* Mol Psychiatry, 2015. **20**(3): p. 320-8.
19. Weaver, I.C., et al., *The methylated-DNA binding protein MBD2 enhances NGFI-A (egr-1)-mediated transcriptional activation of the glucocorticoid receptor.* Philos Trans R Soc Lond B Biol Sci, 2014. **369**(1652).
20. Hendrich, B., et al., *Closely related proteins MBD2 and MBD3 play distinctive but interacting roles in mouse development.* Genes Dev, 2001. **15**(6): p. 710-23.

21. Wood, K.H., et al., *Tagging methyl-CpG-binding domain proteins reveals different spatiotemporal expression and supports distinct functions.* Epigenomics, 2016. **8**(4): p. 455-73.
22. McNaughton, C.H., et al., *Evidence for social anxiety and impaired social cognition in a mouse model of fragile X syndrome.* Behav Neurosci, 2008. **122**(2): p. 293-300.
23. Mineur, Y.S., L.X. Huynh, and W.E. Crusio, *Social behavior deficits in the Fmr1 mutant mouse.* Behav Brain Res, 2006. **168**(1): p. 172-5.
24. Sato, A., et al., *Rapamycin reverses impaired social interaction in mouse models of tuberous sclerosis complex.* Nat Commun, 2012. **3**: p. 1292.
25. Tavares, R.M., et al., *A Map for Social Navigation in the Human Brain.* Neuron, 2015. **87**(1): p. 231-43.
26. Yang, L., et al., *Hypocretin/orexin neurons contribute to hippocampus-dependent social memory and synaptic plasticity in mice.* J Neurosci, 2013. **33**(12): p. 5275-84.
27. Heyward, F.D., et al., *Obesity Weighs down Memory through a Mechanism Involving the Neuroepigenetic Dysregulation of Sirt1.* J Neurosci, 2016. **36**(4): p. 1324-35.
28. Heyward, F.D., et al., *Adult mice maintained on a high-fat diet exhibit object location memory deficits and reduced hippocampal SIRT1 gene expression.* Neurobiol Learn Mem, 2012. **98**(1): p. 25-32.
29. Mineur, Y.S., et al., *Cholinergic signaling in the hippocampus regulates social stress resilience and anxiety- and depression-like behavior.* Proc Natl Acad Sci U S A, 2013. **110**(9): p. 3573-8.
30. Camarena, V., et al., *Disruption of Mbd5 in mice causes neuronal functional deficits and neurobehavioral abnormalities consistent with 2q23.1 microdeletion syndrome.* EMBO Mol Med, 2014. **6**(8): p. 1003-15.
31. Moretti, P., et al., *Learning and memory and synaptic plasticity are impaired in a mouse model of Rett syndrome.* J Neurosci, 2006. **26**(1): p. 319-27.
32. Lu, H., et al., *Loss and Gain of MeCP2 Cause Similar Hippocampal Circuit Dysfunction that Is Rescued by Deep Brain Stimulation in a Rett Syndrome Mouse Model.* Neuron, 2016. **91**(4): p. 739-747.
33. de Bruin, A., et al., *Genome-wide analysis reveals NRP1 as a direct HIF1alpha-E2F7 target in the regulation of motorneuron guidance in vivo.* Nucleic Acids Res, 2016. **44**(8): p. 3549-66.
34. Ghanem, N., et al., *The Rb/E2F pathway modulates neurogenesis through direct regulation of the Dlx1/Dlx2 bigene cluster.* J Neurosci, 2012. **32**(24): p. 8219-30.
35. Aruga, J., *The role of Zic genes in neural development.* Mol Cell Neurosci, 2004. **26**(2): p. 205-21.
36. Gjoneska, E., et al., *Conserved epigenomic signals in mice and humans reveal immune basis of Alzheimer's disease.* Nature, 2015. **518**(7539): p. 365-9.
37. Hirose, Y. and Y. Ohkuma, *Phosphorylation of the C-terminal domain of RNA polymerase II plays central roles in the integrated events of eucaryotic gene expression.* J Biochem, 2007. **141**(5): p. 601-8.
38. Jonkers, I. and J.T. Lis, *Getting up to speed with transcription elongation by RNA polymerase II.* Nat Rev Mol Cell Biol, 2015. **16**(3): p. 167-77.
39. Creyghton, M.P., et al., *Histone H3K27ac separates active from poised enhancers and predicts developmental state.* Proc Natl Acad Sci U S A, 2010. **107**(50): p. 21931-6.
40. Heintzman, N.D., et al., *Histone modifications at human enhancers reflect global cell-type-specific gene expression.* Nature, 2009. **459**(7243): p. 108-12.
41. Pundhir, S., et al., *Peak-valley-peak pattern of histone modifications delineates active regulatory elements and their directionality.* Nucleic Acids Res, 2016. **44**(9): p. 4037-51.
42. McGhee, J.D., et al., *A 200 base pair region at the 5' end of the chicken adult beta-globin gene is accessible to nuclease digestion.* Cell, 1981. **27**(1 Pt 2): p. 45-55.

43. Ludwig, A.K., P. Zhang, and M.C. Cardoso, *Modifiers and Readers of DNA Modifications and Their Impact on Genome Structure, Expression, and Stability in Disease.* Front Genet, 2016. **7**: p. 115.
44. Wang, L., et al., *Mbd2 promotes foxp3 demethylation and T-regulatory-cell function.* Mol Cell Biol, 2013. **33**(20): p. 4106-15.
45. Yin, Y., et al., *Impact of cytosine methylation on DNA binding specificities of human transcription factors.* Science, 2017. **356**(6337).
46. Cukier, H.N., et al., *The expanding role of MBD genes in autism: identification of a MECP2 duplication and novel alterations in MBD5, MBD6, and SETDB1.* Autism Res, 2012. **5**(6): p. 385-97.
47. Gandal, M.J., et al., *Transcriptome-wide isoform-level dysregulation in ASD, schizophrenia, and bipolar disorder.* Science, 2018. **362**(6420).
48. Sanders, S.J., et al., *Insights into Autism Spectrum Disorder Genomic Architecture and Biology from 71 Risk Loci.* Neuron, 2015. **87**(6): p. 1215-1233.
49. Cheishvili, D., et al., *Synergistic effects of combined DNA methyltransferase inhibition and MBD2 depletion on breast cancer cells; MBD2 depletion blocks 5-aza-2'-deoxycytidine-triggered invasiveness.* Carcinogenesis, 2014. **35**(11): p. 2436-46.
50. Shukeir, N., et al., *Alteration of the methylation status of tumor-promoting genes decreases prostate cancer cell invasiveness and tumorigenesis in vitro and in vivo.* Cancer Res, 2006. **66**(18): p. 9202-10.
51. Stefanska, B., et al., *Transcription onset of genes critical in liver carcinogenesis is epigenetically regulated by methylated DNA-binding protein MBD2.* Carcinogenesis, 2013. **34**(12): p. 2738-49.
52. Edalatmanesh, M.A., et al., *Increased hippocampal cell density and enhanced spatial memory in the valproic acid rat model of autism.* Brain Res, 2013. **1526**: p. 15-25.
53. Sosa-Diaz, N., et al., *Prefrontal cortex, hippocampus, and basolateral amygdala plasticity in a rat model of autism spectrum.* Synapse, 2014. **68**(10): p. 468-73.
54. Nicolson, R., et al., *Detection and mapping of hippocampal abnormalities in autism.* Psychiatry Res, 2006. **148**(1): p. 11-21.
55. Courchesne, E., et al., *Neuron number and size in prefrontal cortex of children with autism.* JAMA, 2011. **306**(18): p. 2001-10.
56. Berger, J. and A. Bird, *Role of MBD2 in gene regulation and tumorigenesis.* Biochem Soc Trans, 2005. **33**(Pt 6): p. 1537-40.
57. Nan, X., S. Cross, and A. Bird, *Gene silencing by methyl-CpG-binding proteins.* Novartis Found Symp, 1998. **214**: p. 6-16; discussion 16-21, 46-50.
58. Chahrour, M., et al., *MeCP2, a key contributor to neurological disease, activates and represses transcription.* Science, 2008. **320**(5880): p. 1224-9.
59. Li, C., et al., *MeCP2 enforces Foxp3 expression to promote regulatory T cells' resilience to inflammation.* Proc Natl Acad Sci U S A, 2014. **111**(27): p. E2807-16.
60. Jobe, E.M., et al., *Methyl-CpG-Binding Protein MBD1 Regulates Neuronal Lineage Commitment through Maintaining Adult Neural Stem Cell Identity.* J Neurosci, 2017. **37**(3): p. 523-536.
61. Angrisano, T., et al., *TACC3 mediates the association of MBD2 with histone acetyltransferases and relieves transcriptional repression of methylated promoters.* Nucleic Acids Res, 2006. **34**(1): p. 364-72.
62. Detich, N., J. Theberge, and M. Szyf, *Promoter-specific activation and demethylation by MBD2/demethylase.* J Biol Chem, 2002. **277**(39): p. 35791-4.
63. Cui, Y. and J. Irudayaraj, *Dissecting the behavior and function of MBD3 in DNA methylation homeostasis by single-molecule spectroscopy and microscopy.* Nucleic Acids Res, 2015. **43**(6): p. 3046-55.

64. Vogel Ciernia, A. and J. LaSalle, *The landscape of DNA methylation amid a perfect storm of autism aetiologies.* Nat Rev Neurosci, 2016. **17**(7): p. 411-23.
65. Nardone, S., et al., *Dysregulation of Cortical Neuron DNA Methylation Profile in Autism Spectrum Disorder.* Cereb Cortex, 2017. **27**(12): p. 5739-5754.
66. Richetto, J., et al., *Genome-wide DNA Methylation Changes in a Mouse Model of Infection-Mediated Neurodevelopmental Disorders.* Biol Psychiatry, 2017. **81**(3): p. 265-276.
67. Xie, B., et al., *Genetic association study between methyl-CpG-binding domain genes and schizophrenia among Chinese family trios.* Psychiatr Genet, 2014. **24**(5): p. 221-4.

Figure Legends

Figure 1. Behavioral effects of *Mbd2* deficiency. A. Locomotion in the Open-field box was assessed for 5 min. n=14 wild-type, n=15 mMbd2-/-. B. Exploration time during object-location memory training (left) and discrimination ratio in object-location memory test (right). Discrimination ratio was significantly lower in *Mbd2-/-* mice (Two-way ANOVA, main effect of genotype $F(1,24)=5.05$, $p= 0.0341$; n=13 wild-type, n=15 *Mbd2-/-*). C. Social interaction. Mice were introduced to a novel mouse for 5 min and interaction time was recorded. (Two-way ANOVA, main effect of genotype $F(1,29)=5.02$, $p= 0.0329$; n=17 wild-type, n=16 *Mbd2-/-*). D. Time spent in the light compartment of the Dark-Light Box (left) (Two-way ANOVA, main effect of genotype $F(1,29)=5.3$, $p=0.0287$; n=17 wild-type, n=16 Mbd2-/-) and number of entries to the light side (right). E. Y-maze spontaneous alteration was not affected in *Mbd2-/-* mice (right). SAP-Spontaneous Alteration Performance, AAR-Alternate Arm Return, SAR-Same Arm Return. Exploration is expressed as number of arm entries (left). n=17 wild-type, n=17 *Mbd2-/-*. Data are presented as mean ±SEM *$p<0.05$, for wild-type vs *Mbd2-/-*. ### $p<0.005$ for wild-type over chance (50%) exploration (one-sample t-test). Note: no main effect for sex was observed in any of the tests. Therefore, behavioral data from males and females were collapsed within

genotype for clarity, for full data see Fig S1-S2).

Figure 2. Landscape of Mbd2 binding delineated by ChIP-seq. A. Position of Mbd2 binding peaks Vis-a Vis distance to TSS and their peak fold enrichment. B. Heatmap of the overlap between Mbd2 peaks and the following histone-marks in the hippocampus: H3K4me1, H3K4me3, H3k2me3, H3K27ac, H39Kme3, H3K36me3 and H4K20me1. C. Analysis of the number of Mbd2 peaks located on histone-marks. D. Co-occupancy enrichment analysis of Mbd2 and histone-marks. E. Pathway analysis enrichment of Mbd2 binding peaks (Top 5 pathways are presented). F. Q-ChIP validation of Mbd2 peaks, $p<0.001$. G-H. Q-ChIP for RNApolII(SP5) (G) and H3K4me1 (H). For Q-ChIP of Mbd2, RNApolII(SP5) and H3K4me1 pool of 5-6 mice analyzed by triplicate/group). Data are presented as mean $\pm$SEM *$p<0.05$, ***$p<0.001$ (T-test). TTS-Transcription Termination Site.

Figure 3. Effect of Mbd2 deficiency on gene expression and DNA methylation. A. Heatmap of all transcribed genes in *Mbd2-/-* and wild-type mice sorted by log2 fold-change. B. Pathway analysis enrichment of down-regulated genes (Top 5 pathways are presented). C. Pathway analysis enrichment of up-regulated genes (Top 5 pathways are presented). D. A cumulative distribution of methylation levels of regulatory DNA regions bound by Mbd2 demonstrating hyper-methylation in *Mbd2-/-* hippocampus (K-S test). E. Number of differentially-methylated CpGs (with at least 10% change in methylation and $p<0.001$) in Mbd2-bound annotated genes showing that more CpGs became hyper-methylated then hypo-methylated ($p=0.0339$, binomial test). F. Number of differentially-methylated CpGs (with at least 10% change in methylation and

p<0.001) located within Mbd2-peaks (p<1E-8, binomial test). G. I. Pearson correlation between differential promoter DNA-methylation and gene-expression in *Mbd2-/-* hippocampi.

Figure 4. Overlap between *Mbd2-/-* mice hippocampal transcriptome and human brain transcriptomes in psychiatric disorders. A. Heatmap of log10(p-values) of differentially-expressed gene overlap between *Mbd2-/-* mice and ASD, schizophrenia and bipolar disorder human brain. B. Pearson's correlations of fold-changes in gene-expression levels between *Mbd2-/-* mice and ASD (n=286 genes), schizophrenia (n=686 genes) and bipolar disorder human brain (n=137 genes).

Figure 5. Overlap between down-regulated genes in *Mbd2-/-* mice and ASD-risk genes. A. An overlap analysis revealed a significant intersection between human ASD high risk genes and down-regulated (Top) but not up-regulated (Bottom) genes in *Mbd2-/-* hippocampi. B. An overlap analysis revealed a significant intersection between human ASD risk genes based on the SFARI Gene Project and down-regulated (Top) but not up-regulated (Bottom) genes in *Mbd2-/-*. (Hypergeomtric tests) . C. Western blot analysis showing reduced protein levels of Drd2, Pogz and Zbtb16 in *Mbd2-/-* mice hippocampi. Proteins weights as determined using molecular weight markers are indicated. D. Representative immunofluorescence images of the hippocampus (CA1 layer) in wild-type and *Mbd2-/-* mice showing neuronal nuclei immunoreactivity (NeuN, green immunoreactivity). Scale bar: 100µm. D. Quantification of average neuronal soma size of the CA1 layer. E. Quantification of neuronal cell count in CA1 layer. F. Reverse correlation between average neuronal soma size and neuronal cell count (Pearson's r=-0.7265, p=0.0266). G. Average thickness of CA1 layer. Data are presented as mean ±SEM. *p<0.05, **p<0.01 (t-tests and U-test for (G)); n=4-5/group.

Figure 6. Virus-mediated Mbd2 down-regulation. A. shMbd2 viral construct reduces *Mbd2* mRNA. Mbd2 mRNA levels were reduced in the hippocampus from shMbd2-infused mice compared with scramble control-infused mice. Scramble n=6, sh*Mbd2* n=4 (T test). B. Representative micrograph of Mbd2 immunolabeling in hippocampal slices from Scramble- and sh*Mbd2*- infused mice. Scale bar: 200µm. C. Locomotion in Open-field box. D. Discrimination ratio in object-location memory test. E. Social interaction test. F. Time in the light compartment of the Dark-Light Box (left) and number of entries to the light side (right). Data are presented as mean ±SEM *p<0.05, for wild-type vs *Mbd2-/-* (t-test). # p<0.05 for wild-type over chance (50%) exploration (one-sample t-test). Scramble n=7, shMbd2 n=6.

Supplementary figures legend

Supplementary Figure 1. A. Behavioral analyses of male and female *Mbd2-/-* and control mice A. Locomotion in Open-field box was assessed for 5 min. B. Number of entries to center in the open-field test. C. Average speed during the open-field test. D. Social interaction, mice were introduced to a novel mouse for 5 min and interaction time was recorded. E. Exploration time during object-location memory training and F. Discrimination ratio in object-location memory test. G. Time in the light compartment of the Dark-Light Box and H. number of entries to the light side. Numbers within bars represent sample size.

Supplementary Figure 2. Top: Y-maze spontaneous alteration. SAP-Spontaneous Alteration Performance, AAR-Alternate Arm Return, SAR-Same Arm Return, B. Bottom: Exploration is expressed as number of arm entries. Numbers within bars represent sample size.

Supplementary Figure 3. Average speed (left), entries to center (right) in the open-field box test. p>0.05 in all cases.

Supplementary Figure 4. A. Histogram of Mbd2 binding peaks around Transcription start sites (TSS) B. Top De-novo motif discovery sequences found in HOMER analysis.

Supplementary Figure 5. A. GO-Pathway analysis enrichment of Mbd2-bound genes. B. Gene-network analysis of Mbd2 binding peaks.

Supplementary Figure 6. A. A capture from genome browser showing RNA-seq read alignments for the first 3 exons of the *Mbd2* gene. *Mbd2-/-* mice show expression of the first exon only, as expected by the design of this mouse line [20]. **B.** QPCR validation for up-regulated genes (*Apba2, Kcnd2, Clstn1, Gria3a, Jarid2, Gria1*) and down-regulated genes (*Ttr*, *Aqp1*, *Rdh5*) shows change in gene-expression in *Mbd2-/-* mice in agreement with the RNA-Seq data (n=9 wild-type, n=6 *Mbd2-/-*; *p<0.05, t-test).

Supplementary Figure 7. A. GO-Pathway analysis enrichment of *Mbd2-/-* down-regulated genes. B. Gene-network analysis *Mbd2-/-* down-regulated genes.

Supplementary Figure 8. A. GO-Pathway analysis enrichment of *Mbd2-/-* up-regulated genes. B. Gene-network analysis *Mbd2-/-* up-regulated genes.

Supplementary Figure 9. A. GO-pathway meta-analysis of the overlapping ChIP-seq and RNA-seq gene-pathways by unsupervised clustering. B. Circus plot depicting the relation between gene represented in CHIP-seq and RNA-Seq experiments, showing stronger connection between Mbd2 peaks and down-regulated genes in comparison with up-regulated genes.

Purple lines link shared genes across gene-lists, blue lines link different genes which fall into the same ontology term.

Supplementary Figure 10. Effect of *Mbd2-/-* on gene expression of epigenetic readers and modifiers. *FDR-corrected p<0.05, **FDR-corrected p<0.01, #FDR-corrected p<0.1. Note: Mbd2-aligned reads in *Mbd2-/-* mice are from the intact exon 1 (see also Fig S6A).

Supplementary Figure 11. A. A table summarizing the number of differentially-methylated CpGs and genes under the different analytical conditions. B. A capture from IGV genomic browser depicting Mbd2 binding peak around Sfi1 transcription start site (TSS) with methylation levels and differential-methylation between wild-type and *Mbd2-/-* mice hippocampus. C. cumulative distribution of methylation levels of regulatory DNA regions genome-wide demonstrating hyper-methylation in *mbd2-/-* hippocampus (K-S test). D. Significant motifs discovered for promoter CpG with positive correlation between DNA methylation and gene-expression are depicted. No significant motifs were found for CpGs with negative correlation between DNA methylation and gene-expression. E-F. Pathway analysis of hypo- (E) and hyper- (F) methylated gene promoters.

Supplementary Figure 12. A. Correlation analysis of CpG methylation levels in capture-array genome-wide bisulfite-sequencing and amplicons bisulfite-sequencing for wild-type mice. B. Correlation analysis of CpG methylation levels in capture-array genome-wide bisulfite-sequencing and amplicons bisulfite-sequencing for wild-type mice. C. Average change in methylation levels across all CpGs (with at least 1% change in methylation) show larger change in methylation between Mbd2-/- and wild-type mice in CpGs that became hyper-methylated

(n=114) than in CpGs that became hypo-methylated (n=80) (t-test, **p<0.01) D. More CpGs with at least 1% change in methylation between mbd2-/- and wild-type mice are hyper-methylated than hypo-methylated (binomial test, *p<0.05). E. A cumulative distribution of methylation levels within Mbd2 peak regions in a validation cohort (K-S test).

Supplementary Figure 13. A-B. Protein-Protein Interaction Networks for down- (A) and up- (B) regulated genes overlapped with ASD risk genes (Sanders et al[48]). PPI=Protein-Protein Interaction.

Supplementary Figure 14. A-B. Protein-Protein Interaction Networks for down- (A) and up- (B) regulated genes in *Mbd2-/-* overlapped with SFARI-GENE dataset. PPI=Protein-Protein Interaction. Disconnected nodes are omitted from (A) for clarity.

Supplementary Figure 15. A. Neuron count (left), average neuron size (middle) and layer thickness (right) of hippocampi CA2 layer in wild-type and *Mbd2-/-* mice as determined by quantitative analyses following NeuN immunolabeling. Representative pictures are provided in the far left. B. Neuron count (left), average neuron size (middle) and layer thickness (right) of the hippocampus CA3 layer C. Correlation analyses between neuronal size and layer thickness (left) and between neuron count and thickness (right) of the CA1 layer. D. Correlation analyses between neuronal size and layer thickness (left), between neuron count and average neuronal size (middle) and between neuron count and thickness (right) of the CA2 layer. E. Correlation analyses between neuronal size and layer thickness (left), between neuron count and average neuronal size (middle) and between neuron count and thickness (right) of the CA3 layer. F. Correlation analyses between neuronal size and layer thickness (left), between neuron count

and average neuronal size (middle) and between neuron count and thickness (right) of the total hippocampus (collapsing CA1, CA2 and CA3 data). *p<0.05, t-tests for between group comparisons. Pearson's Rs for linear correlation analyses, with exact p-values indicated in each graph.

Supplementary Figure 16. A. Schematic illustration of the sh-*Mbd2*/scramble constructs. RRE-Rev Response Element, hCMV-human Cytomegalovirus promoter, tGFP-turbo GFP reporter, IRES-Internal Ribosomal Entry Site, PURO^{R}-Puromycin Resistance, WPRE-Woodchuck Hepatitis Posttranslational Regulatory Element. B-C. In-vitro validation of sh-*Mbd2* construct. The effect of sh-*Mbd2* constructs on Mbd2 mRNA levels and protein levels in lentivirus-treated NIH3T3 was tested by qRT-PCR (B) and Western blot (C) respectively (change over scramble control). D. Illustration of infusion site adapted from the Paxinos and Franklin mouse brain atlas (top) and confocal fluorescence microscope images showing hippocampus expression of GFP-tagged lentivirus (green), MBD2 (red) and a merged image (center), scale bar: 200µm; and larger magnification of lentivirus-infected neurons (bottom), scale bar: 50 µm.

Fig.1

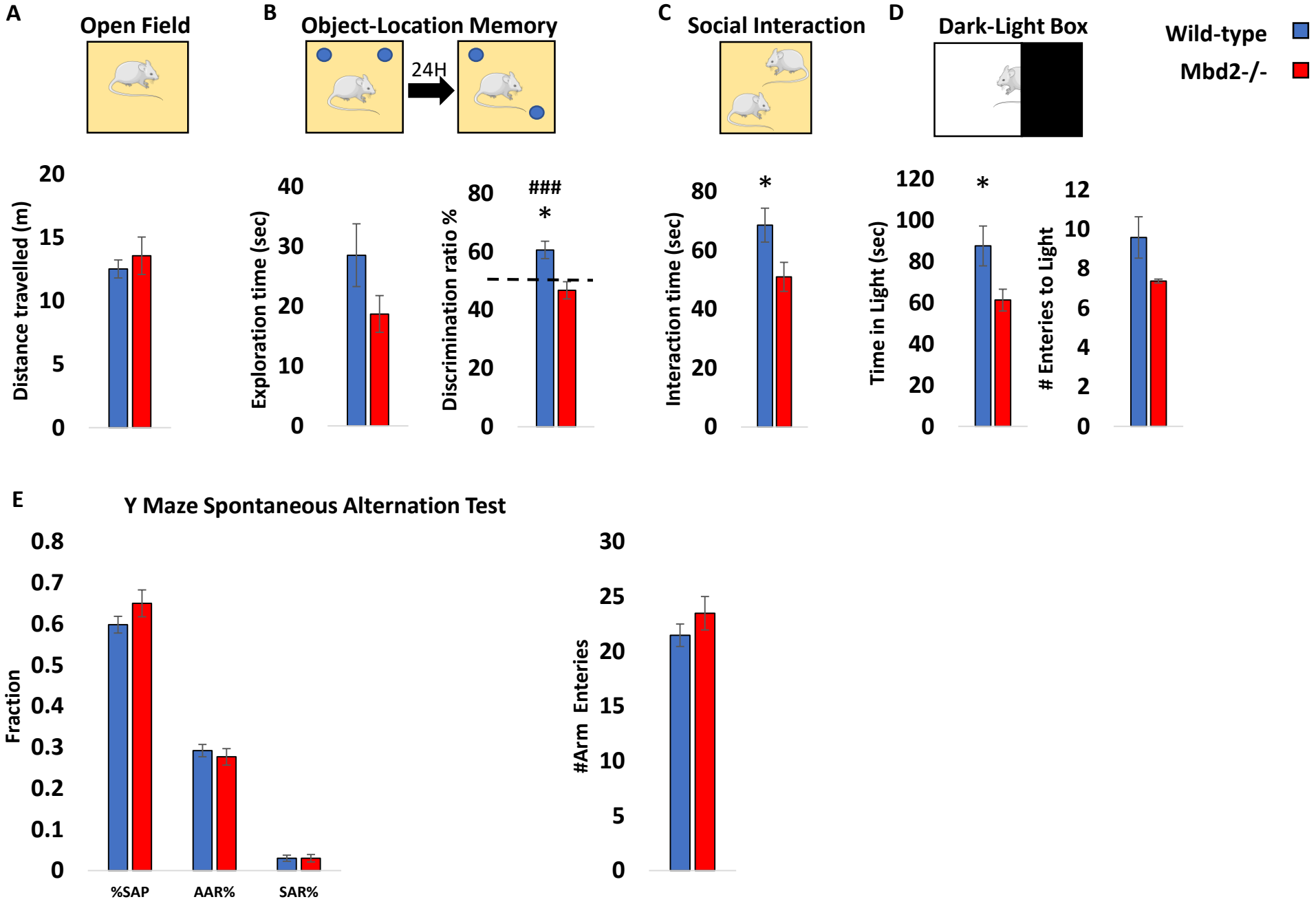
A
Open Field
B
Object-Location Memory
24H
C
Social Interaction
D
Dark-Light Box
Wild-type
Mbd2-/-
Distance travelled (m)
Exploration time (sec)
Discrimination ratio %
###
*
Interaction time (sec)
*
Time in Light (sec)
*
Enteries to Light
E
Y Maze Spontaneous Alternation Test
Fraction
%SAP
AAR%
SAR%
#Arm Enteries

Fig.2

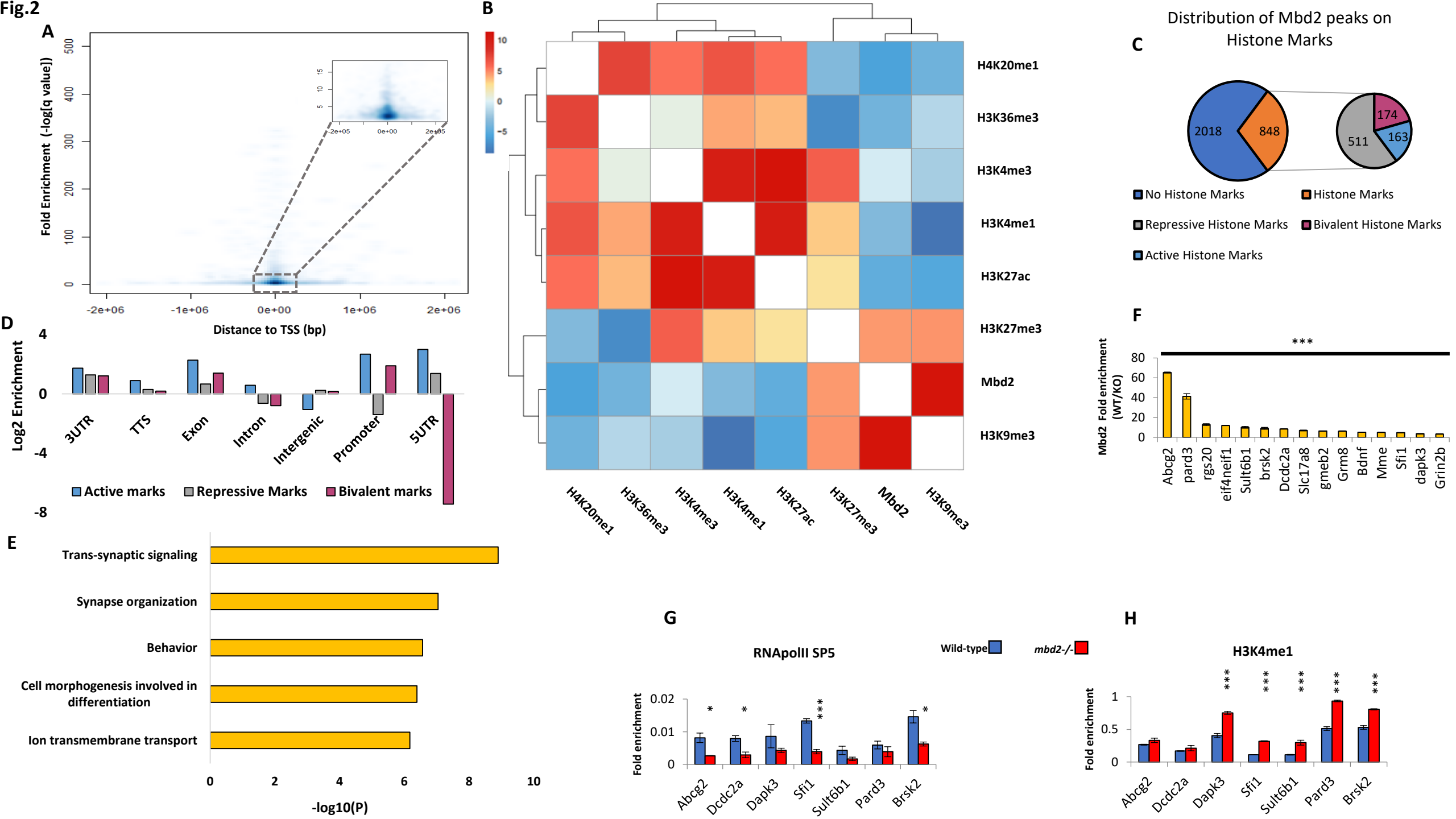
A
Fold Enrichment (-log[q value])
Distance to TSS (bp)
B
H4K20me1
H3K36me3
H3K4me3
H3K4me1
H3K27ac
H3K27me3
Mbd2
H3K9me3
C
Distribution of Mbd2 peaks on Histone Marks
2018
848
511
174
163
No Histone Marks
Histone Marks
Repressive Histone Marks
Bivalent Histone Marks
Active Histone Marks
D
Log2 Enrichment
3UTR
TTS
Exon
Intron
Intergenic
Promoter
5UTR
Active marks
Repressive Marks
Bivalent marks
E
Trans-synaptic signaling
Synapse organization
Behavior
Cell morphogenesis involved in differentiation
Ion transmembrane transport
-log10(P)
F
Mbd2 Fold enrichment (WT/KO)
***
Abcg2
pard3
rgs20
eif4neif1
Sult6b1
brsk2
Dcdc2a
Slc17a8
gmeb2
Grm8
Bdnf
Mme
Sfi1
dapk3
Grin2b
G
RNApolII SP5
Wild-type
mbd2-/-
Fold enrichment
Abcg2
Dcdc2a
Dapk3
Sfi1
Sult6b1
Pard3
Brsk2
H
H3K4me1
Fold enrichment
Abcg2
Dcdc2a
Dapk3
Sfi1
Sult6b1
Pard3
Brsk2

Fig. 3

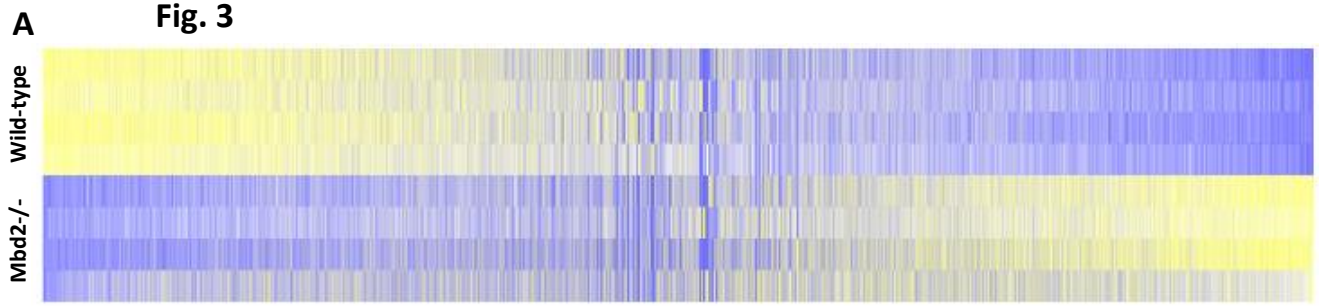
A
Wild-type
Mbd2-/-

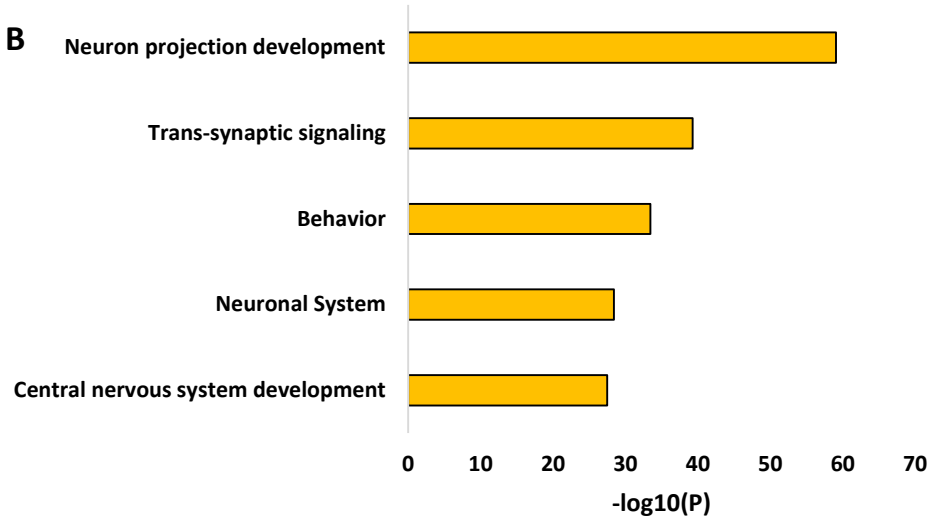
B
Neuron projection development
Trans-synaptic signaling
Behavior
Neuronal System
Central nervous system development
0
10
20
30
40
50
60
70
-log10(P)

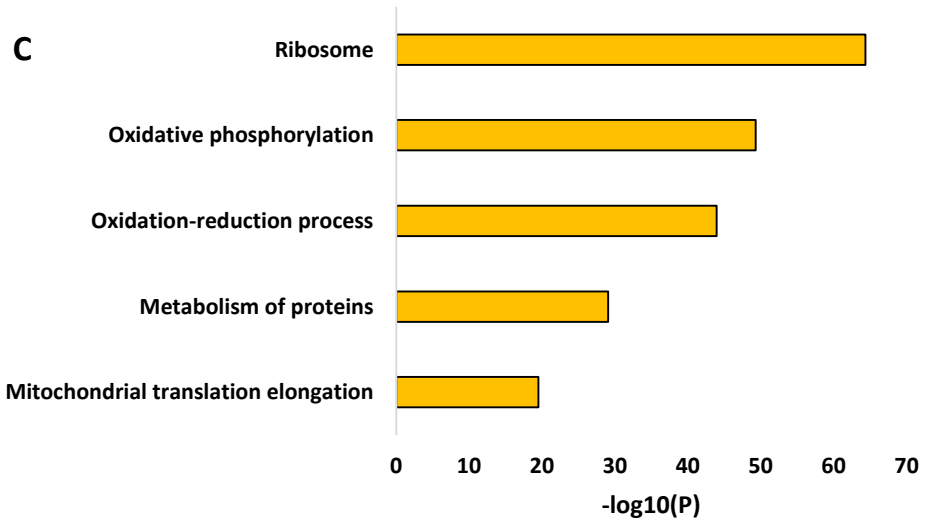
C
Ribosome
Oxidative phosphorylation
Oxidation-reduction process
Metabolism of proteins
Mitochondrial translation elongation
0
10
20
30
40
50
60
70
-log10(P)

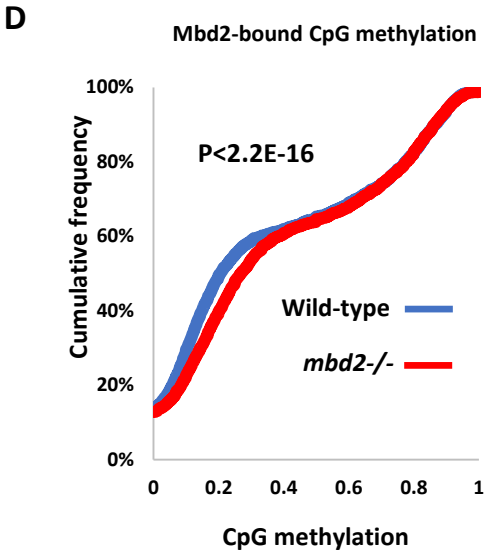
D
Mbd2-bound CpG methylation
100%
80%
60%
40%
20%
0%
Cumulative frequency
P<2.2E-16
Wild-type
mbd2-/-
0
0.2
0.4
0.6
0.8
1
CpG methylation

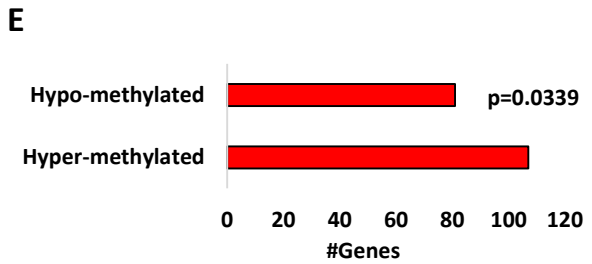
E
Hypo-methylated
Hyper-methylated
p=0.0339
0
20
40
60
80
100
120
#Genes

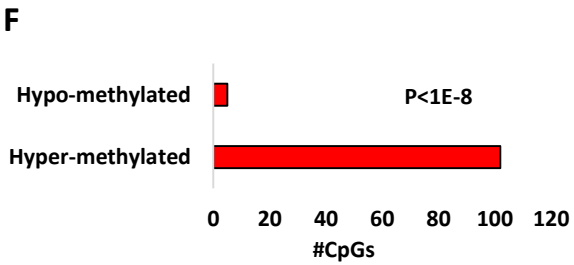
F
Hypo-methylated
Hyper-methylated
P<1E-8
0
20
40
60
80
100
120
#CpGs

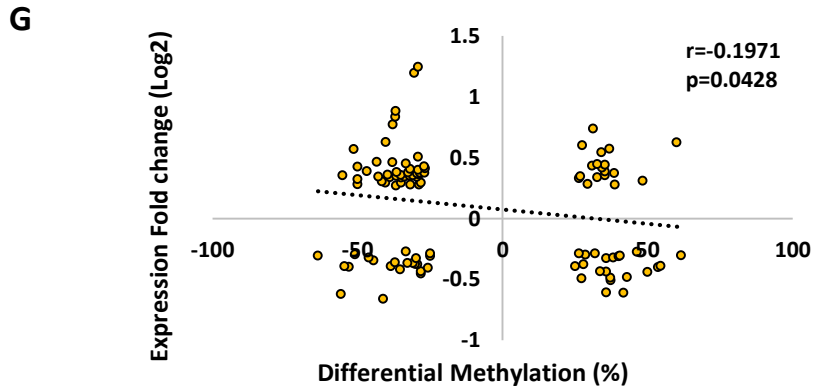
G
1.5
1
0.5
0
-0.5
-1
-100
-50
0
50
100
Expression Fold change (Log2)
r=-0.1971
p=0.0428
Differential Methylation (%)

Fig 4

A

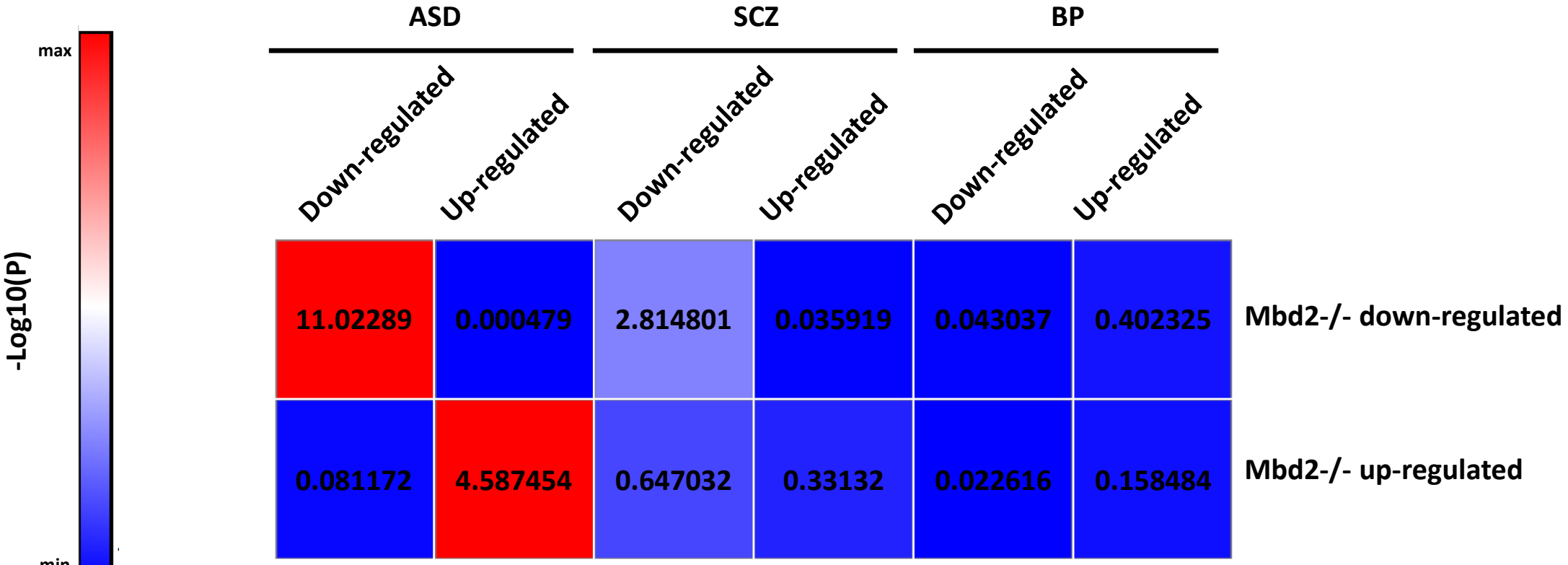
max
min
-Log10(P)
ASD
SCZ
BP
Down-regulated
Up-regulated
Down-regulated
Up-regulated
Down-regulated
Up-regulated
11.02289
0.000479
2.814801
0.035919
0.043037
0.402325
Mbd2-/- down-regulated
0.081172
4.587454
0.647032
0.33132
0.022616
0.158484
Mbd2-/- up-regulated

B

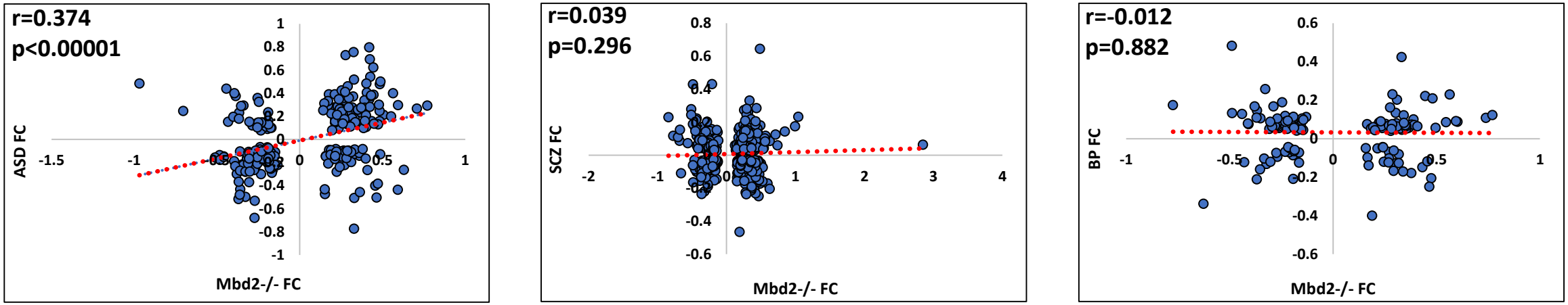
r=0.374
p<0.00001
ASD FC
Mbd2-/- FC
r=0.039
p=0.296
SCZ FC
Mbd2-/- FC
r=-0.012
p=0.882
BP FC
Mbd2-/- FC

Fig.5

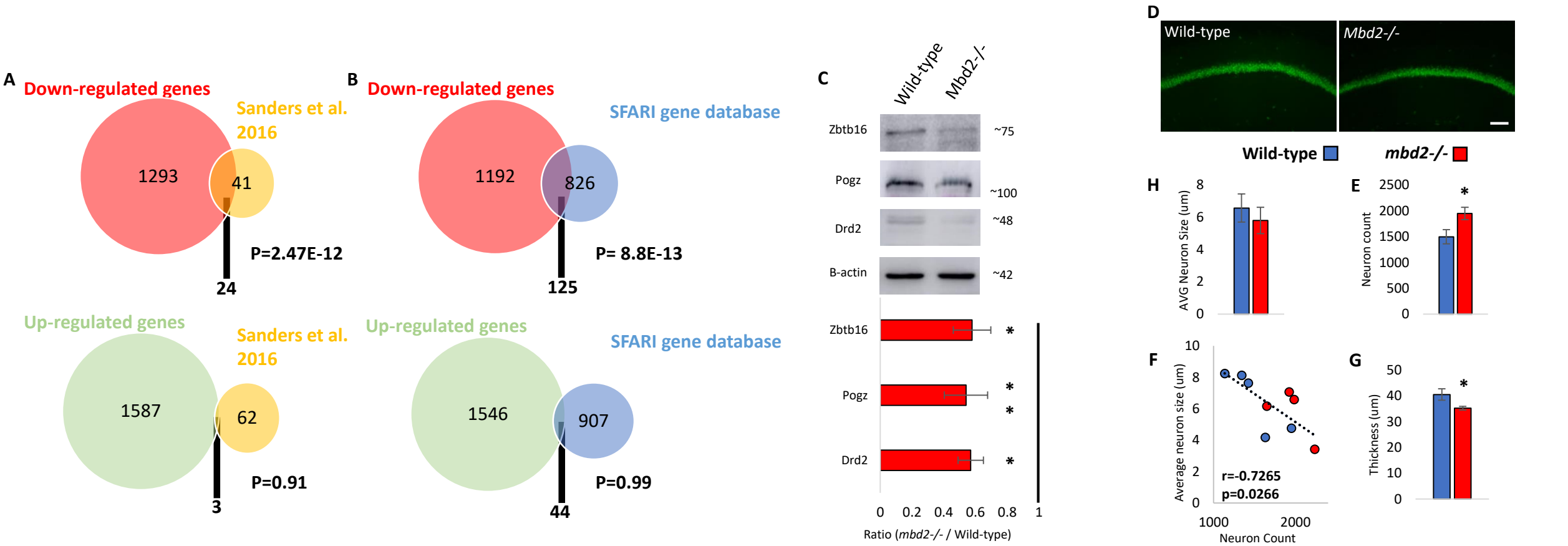
A
Down-regulated genes
Sanders et al. 2016
1293
41
P=2.47E-12
24
Up-regulated genes
Sanders et al. 2016
1587
62
P=0.91
3
B
Down-regulated genes
SFARI gene database
1192
826
P= 8.8E-13
125
Up-regulated genes
SFARI gene database
1546
907
P=0.99
44
C
Wild-type
Mbd2-/-
Zbtb16
~75
Pogz
~100
Drd2
~48
B-actin
~42
Zbtb16
Pogz
Drd2
0 0.2 0.4 0.6 0.8 1
Ratio (mbd2-/- / Wild-type)
D
Wild-type
Mbd2-/-
Wild-type
mbd2-/-
H
AVG Neuron Size (um)
E
Neuron count
F
Average neuron size (um)
r=-0.7265
p=0.0266
1000 2000
Neuron Count
G
Thickness (um)

Fig.6

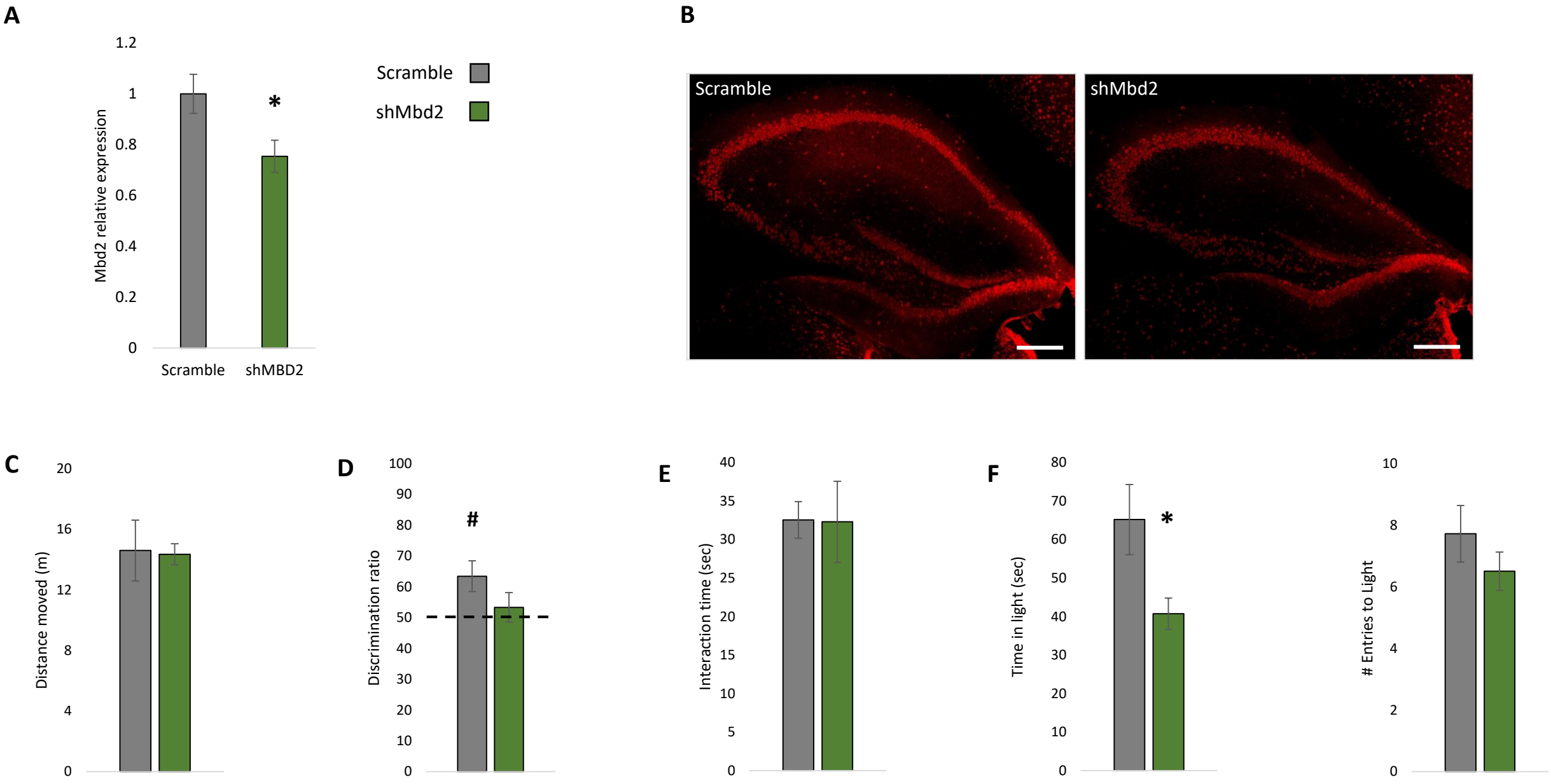
A
1.2
1
0.8
0.6
0.4
0.2
0
Mbd2 relative expression
*
Scramble
shMBD2
Scramble
shMbd2
B
Scramble
shMbd2
C
20
16
12
8
4
0
Distance moved (m)
D
100
90
80
70
60
50
40
30
20
10
0
Discrimination ratio
#
E
40
35
30
25
20
15
10
5
0
Interaction time (sec)
F
80
70
60
50
40
30
20
10
0
Time in light (sec)
*
10
8
6
4
2
0
Entries to Light